Journal of Peptide Science
J. Peptide Sci. **8**: 621–633 (2002)
Published online in Wiley InterScience (www.interscience.wiley.com). DOI: 10.1002/psc.422

Synthesis of Complex Phosphopeptides as Mimics of p53 Functional Domains

GYORGYI VARADI* and LASZLO OTVOS JR

The Wistar Institute, 3601 Spruce Street, Philadelphia, Pennsylvania 19104, USA

Received 20 June 2002
Accepted 25 June 2002

Abstract: A complete set of mono-, di- and triphosphorylated peptides comprising amino acids 10–27, the Mdm2 and p300 binding site(s) of p53, with and without a fluorescein label at the *N*-terminus, was synthesized by step-by-step solid phase synthesis. Fluorescence polarization analysis revealed that phosphorylation at Thr^{18} decreased binding to recombinant Mdm2 protein compared with the unphosphorylated and the two other single phosphorylated analogues. Unlabelled multiply phosphorylated peptides corresponding to this amino-terminal transactivation domain proved to be powerful tools in analysing the phosphate specificity of existing anti-p53 monoclonal and polyclonal antibodies using direct ELISA. The tetramerization domain of human p53 protein was modelled with a 53 residue-long unlabelled unphosphorylated and Ser^{315}-phosphorylated peptide pair. CD analysis showed similar α-helical structures for both peptides and no major difference in the secondary structure could be observed upon phosphorylation. Size-exclusion HPLC indicated that these synthetic oligomerization domain mimics underwent a pH-dependent tetramerization process, but the presence of a phosphate group at Ser^{315} did not modify the oligomeric state of the 308–360 p53 fragments. Nevertheless, the fluorescein-labelled Ser^{315} phosphorylated peptide bound to the downstream signalling ligand DNA topoisomerase I protein with slightly higher affinity than did the unphosphorylated analogue. Copyright © 2002 European Peptide Society and John Wiley & Sons, Ltd.

Keywords: p53; synthetic peptide; phosphorylation; fluorescence polarization; tetramerization; size-exclusion HPLC

INTRODUCTION

The tumour suppressor p53 protein is present at very low levels in normally growing cells. Different types of cellular stress, including DNA damage, hypoxia and inappropriate oncogene signaling initiate accumulation of the expressed gene product [1–5]. Activation of p53 leads to either cell-cycle arrest, or apoptosis, events that contribute to the genomic integrity in eukaryotic cells [6–9]. Phosphorylation is one of the key regulatory steps in the activation process of p53 protein [10]. Genotoxic stresses activate many cellular kinases that phosphorylate various serine and threonine residues in the independently functioning *N*-terminal and *C*-terminal domains [11].

It is known now that the *N*-terminal domain plays a crucial role in p53 function. This domain is responsible for the transactivation properties of p53 [12] and binding to such regulatory proteins as the inhibitor Mdm2 [13] and its human analogue Hdm2 or the positive effector p300. Phosphorylation at Ser^{15}, Thr^{18} and Ser^{20} appears to have an impact on association of p53 with Mdm2 [14,15] or p300 [16,17]. However, different laboratories reported slightly different or controversial results on the role of specific phosphorylation sites in these interactions. Most of these studies used modified full-length or truncated p53 proteins for the

*Correspondence to: Dr Gyorgyi Varadi, Department of Medical Chemistry, University of Szeged, Dom ter 8, H-6720, Szeged, Hungary; e-mail: varadigy@mdche.szote.u-szeged.hu
Contract/grant sponsor: NIH; Contract/grant number: GM 55860.

Copyright © 2002 European Peptide Society and John Wiley & Sons, Ltd.

investigation of the association. A possible explanation of the disagreement emerged from the study of Dumaz *et al.* [18], is that the relative levels of p53 and Mdm2 or p300 expression are essential for the phosphorylation process and for observing the ensuing physiological effects. To overcome this problem and the difficulty of the production of specifically phosphorylated derivatives of the whole p53 protein, several laboratories used phosphopeptides for representing the *N*-terminal sub-domain of p53. Biotinylated peptides were involved in ELISA binding analysis [19] and fluorescein-labelled fragments were used in fluorescence polarization experiments [20,21]. Although it is to be determined whether phosphorylation at a single amino acid alone is sufficient to induce or inhibit interaction of p53 with regulatory proteins [22], none of the previous studies used a complete set of mono-, di- and tri-phosphorylated peptides representing the Mdm2 and p300 binding site(s) of p53. A straightforward direct assay would require the preparation of peptides carrying fluorescein at the *N*-terminus (as the analogues of the 5′-labelled oligonucleotides in the successful binding experiment of the *C*-terminal domain of p53 and DNA [23]) and phosphate groups at different side-chain positions in all possible combinations. In addition, a series of unlabelled phosphopeptides would be the most powerful tool for the analysis of the specificity of antibodies raised against phosphate esters of Ser^{15}, Thr^{18} and Ser^{20}.

The *N*-terminal domain is one of the most important regions of p53 at which interactions with regulatory proteins take place. Additional proteins and biopolymers bind to different parts of p53, most notably to the *C*-terminus. The interaction domain with DNA topoisomerase I, a multifunctional enzyme whose enzymatic activity is stimulated by p53 [24], is located to the beginning of the tetramerization domain [25]. Intriguingly, Ser^{315}, the $p34^{Cdc2}$/clb kinase site [26] falls right in this region. It is highly conceivable that excessive phosphorylation of Ser^{315} by $p34^{Cdc2}$/clb kinase, or the lack of dephosphorylation by the Cdc14 phosphatase [27], will interfere with the p53-DNA topoisomerase I interaction. This hypothesis can be investigated by fluorescein-labelled peptides representing the phosphorylated and unphosphorylated variants of the extended tetramerization domain of p53 protein.

Wild-type p53 undergoes oligomerization and can assume two distinct conformational states, with either low (monomer) or high (oligomer) affinity for site-specific DNA binding [28]. A detailed study using a set of synthetic peptides corresponding to wild-type p53 determined that the 319–360 core peptide exhibits the strongest affinity for tetramerization [29]. The tetramerization domain of p53 consists of a largely unordered region between amino acid residues 319 and 323, followed by a turn centred at residues 324 and 325, a short β-pleated sheet between residues 326 and 333, a Gly^{334} residue that breaks the ordered structure, an α-helix at residues 335–356 and a *C*-terminal flanking region between residues 357 and 360 [30]. The tetramer is formed first by antiparallel assembly of the β-sheets of two units, followed by the association of the α-helical domains of two dimers. In this model, phosphorylation of Ser^{315} can conceivably interfere with tetramer assembly by forming an ionic bridge with a positively charged residue in the neighbourhood of the end of the α-helix, and disturbing the fine balance and orientation of the ordered segments. Since inhibition of the tetramer formation upon mutations of three amino acid residues in the oligomerization domain was elegantly shown using peptides and size-exclusion HPLC [31], unphosphorylated and Ser^{315} phosphorylated fragments of the extended tetramerization domain of p53 can be used for the investigation of the oligomerization process by size-exclusion chromatography.

The primary aim of this study was the synthesis of a complete set of fluorescein-labelled phosphopeptides from the Mdm2/Hdm2 and p300 as well as DNA topoisomerase I binding sites of p53. In addition, we synthesized the peptides without labelling for enzyme-linked immunosorbent assay against phosphate-specific antibodies and for size-exclusion chromatographic analysis of the tetramerization domain.

MATERIALS AND METHODS

Peptide Synthesis

Peptides were synthesized on Rainin PS3 and Milligen 9050 automatic synthesizers, applying Fmoc chemistry and HATU coupling in *N*-methylpyrrolidone with a twofold excess of reagents. TentaGel SRamFmoc resin (Advanced ChemTech, Inc., Louisville, KY) was used as a solid support. Side-chain protection was afforded by *tert*-butyl esters and ethers for Asp, Glu, Ser, Thr and Tyr, Boc for Lys and Trp, Trt for Asn and Gln and Pmc for Arg. Phosphoserine and phosphothreonine residues were

Copyright © 2002 European Peptide Society and John Wiley & Sons, Ltd.

incorporated as Fmoc-Ser(PO_3HBzl)-OH or Fmoc-Thr(PO_3HBzl)-OH, purchased from Novabiochem Ltd. (San Diego, CA) and using double coupling. Fluorescence labelling was performed manually on the solid support using a tenfold excess of 5(6)-carboxyfluorescein (Sigma, St Louis, MO) and DIC/HOBt activation with a tenfold excess of both reagents in the presence of 1 equivalent of *N*,*N*-diisopropylethylamine. The reaction was conducted until the ninhydrin test failed to reveal remaining free amino groups on the *N*-termini [33]. Peptides and phosphopeptides were detached from the resin with a 94 : 5 : 1 (v/v/v) TFA/ thioanisole/water mixture at room temperature for 2 h. The resin was removed and the peptides were precipitated by addition of ice-cold diethyl ether. The precipitated peptides were collected by filtration and dried *in vacuo*.

Purification

Peptides were purified by preparative reversed phase high-performance liquid chromatography (RP-HPLC), using a Beckman System-Gold multisolvent delivery system (Beckman, San Ramon, CA) connected to a photodiode array detector. A 10 × 250 mm Vydac 218 TP column packed with C18 silica gel (300 Å pore diameter, 5 μm particle size; Hesperia, CA) was used. The peptides were eluted with a solvent system of (A) 0.1% TFA in water and (B) 0.1% TFA in acetonitrile at a flow-rate of 3 ml/min. The absorbance was detected at 220 and 280 nm. The appropriate fractions were pooled and lyophilized.

Peptide Characterization

The purity of the peptides was characterized by analytical RP-HPLC, using a 4.6 × 250 mm Vydac 218 TP C18 silica gel packed column (300 Å pore diameter, 5 μm particle size) at a flow-rate of 1 ml/min. The integrity of the peptides was verified by matrix-assisted laser desorption ionization spectrometry (MALDI MS) (MS Facility, The Wistar Institute, Philadelphia, PA). The concentration of the peptide solutions was determined by analytical RP-HPLC calculating the average of three measurements.

Fluorescence Polarization

Binding of the p53 peptides to the regulatory proteins was assessed by fluorescence polarization. For these experiments, the unlabelled binding partner proteins were serially diluted in phosphate-buffered saline (pH 6.8) in a 50 μl final volume in 6 × 50 mm disposable glass borosilicate tubes. The fluoresceinated peptides were added to each tube in 50 μl aliquots to a concentration of 1 nM and the tubes were incubated at 25 °C for 30 min. The extent of fluorescence anisotropy was measured on a Beacon 2000 instrument (Pan Vera, Madison, WI). The filters used were 485 nm excitation and 535 nm emission with 3 nm band width.

Enzyme-Linked Immunosorbent Assay

Anti-phospho-p53 Ser^{15} and Ser^{20} polyclonal (catalogue number 9284 and 9287) and anti-phospho-p53 Ser^{15} 16G8 monoclonal (catalogue number 9286) antibodies were purchased from the Cell Signaling Technology, Inc. (Beverly, MA). Standard 96-well microtitre plates (Maxisorp, Nunc, Roskilde, Denmark) were incubated overnight at 37 °C with 50 μl of a 0.02 mg/ml solution of the peptides in water to allow the antigen to dry onto the surface of the plate. Excess binding sites were blocked with 10% gamma-globulin (GG) free horse serum (Gibco, Gaithersburg, MD) in PBS (100 μl/well) at 37 °C for 2 h. The blocking solution was removed by applying vacuum. One hundred μl of serum diluted to 1/100 and 1/1000 with 10% GG-free horse serum in PBS was added in duplicates and the mixture was incubated overnight at 4 °C. Plates were washed four times with PBS, incubated for another 90 min at 37 °C with 100 μl of HRP-conjugated anti-rabbit (for polyclonal antibodies) or anti-mouse (for the monoclonal antibody) IgG secondary antibodies (Sigma, St Louis, MO), diluted to 1/1000 with PBS. The plates were washed five times in PBS and vacuum dried. One hundred μl of TMB Microwell peroxidase (Kirkegaard and Perry Laboratories, Gaithersburg, MD) was added to the wells. The reaction was stopped after 10 min by adding 100 μl of 1 M phosphoric acid. The ultraviolet absorbance was read at 450 nm on a microtitre plate reader.

Circular Dichroism Spectroscopy

CD spectra were taken on a Jasco J720 instrument at room temperature in a 0.2 mm path length cell. Doubly distilled water and spectroscopy grade trifluoroethanol were used as solvents. The peptide concentrations were 0.2 mg/ml, determined each time by quantitative RP-HPLC. Curves were smoothed by the algorithm provided by Jasco. Mean residue ellipticity ($[\Theta]$) is expressed in deg·cm^2/dmol by using mean residue masses of 114.4 Da (306–360;nP) and 115.9 Da (308–360;315P), based on the actual molecular masses of the peptides.

Copyright © 2002 European Peptide Society and John Wiley & Sons, Ltd.

Table 1 Synthetic Peptides

Peptide	Sequence
10–27;nP	VEPPLSQETFSDLWKLLP
10–27;15P	VEPPLS(*P*)QETFSDLWKLLP
10–27;18P	VEPPLSQET(*P*)FSDLWKLLP
10–27;20P	VEPPLSQETFS(*P*)DLWKLLP
10–27;15,18PP	VEPPLS(*P*)QET(*P*)FSDLWKLLP
10–27;15,20PP	VEPPLS(*P*)QETFS(*P*)DLWKLLP
10–27;18,20PP	VEPPLSQET(*P*)FS(*P*)DLWKLLP
10–27;15,18,20PPP	VEPPLS(*P*)QET(*P*)FS(*P*)DLWKLLP
308–360;nP	
LPNNTSSSPQPKKKPLDGEYFTLQIRGRERFEMFRELNEALELKDAQAGKEPG	
308–360;315P	
LPNNTSSS(P)PQPKKKPLDGEYFTLQIRGRERFEMFRELNEALELKDAQAGKEPG	

Size-Exclusion Chromatography

A Bio-Sil SEC 125-5 column (BioRad Laboratories, Inc., Hercules, CA) was used on a Beckman System-Gold multisolvent delivery system (Beckman, San Ramon, CA) connected to a photodiode array detector. A molecular weight standard purchased from the BioRad Laboratories (Hercules, CA) was used to calibrate the column. Freshly lyophilized samples of the p53 peptides were incubated in buffers at different pH for 30 min, and were loaded on the column.

RESULTS

Peptide Design and Synthesis

A complete set of phosphopeptides was synthesized representing the Mdm2/Hdm2 and p300 binding site of the *N*-terminal domain of p53. Two different requirements were taken into account in the sequence design. Firstly, the fragments had to contain the Mdm2/Hdm2 and p300 binding site(s) of p53 together with Ser^{15}, Thr^{18} and Ser^{20}, the three crucial phosphorylation sites of this region. Secondly, we planned to label the peptides at the amino termini with fluorescein. The fluorescein-label has to be placed somewhat, but not very, far from the expected site of interaction. If the label is exceedingly far, no, or a very weak, polarization signal can be detected. If the label is very close, it will interfere with binding. In our experience a distance of 5–10 amino acids is optimal. Keeping in mind these considerations, the 10–27 fragment of the *N*-terminal domain was synthesized in all possible single, double and triple phosphate forms. The sequences of the peptides are shown in Table 1.

The peptides were prepared on a 0.1 mmol scale as described in the Materials and Methods section. After preliminary experiments that resulted in high levels of impurity of the crude products, a very efficient coupling method, HATU activation, was chosen for the syntheses. Phosphoserine and phosphothreonine were incorporated as *N*-α-Fmoc-*O*-benzyl-phosphoserine or *N*-α-Fmoc-*O*-benzyl-phosphothreonine. Once these monoprotected residues are built in the peptide chain, they are stable to piperidine, the reagent used for cleaving the Fmoc-group after each coupling step. However, incorporation of the multiply protected phosphoamino acids is somewhat slower than that of unphosphorylated amino acids. Formation of deletion sequences could be reduced by using double coupling and a longer reaction time for these amino acids. After each synthesis, three quarters (0.075 mmol) of the peptides were detached from the resin. The cleavage mixture, containing 5% thioanisole and 1% water in TFA, was effective enough to remove all side-chain protecting groups and to protect the tryptophan residue from oxidation. The *N*-terminal free amino group of one quarter (0.025 mmol) of the peptides was labelled with fluorescein on the resin. 5(6)-carboxy-fluorescein was activated with DIC/HOBt in the presence of a tertiary base to keep the amino group unprotonated according to Weber *et al.* [32]. The reaction was performed manually and its progress was followed with the ninhydrin test. Once the test showed near-complete coupling, the labelled peptides were

Copyright © 2002 European Peptide Society and John Wiley & Sons, Ltd.

Table 2 Analytical Properties of the Peptides

Peptide	Formula	MW (Da)		RT[a]
		Calculated	Found	
10–27;nP	$C_{99}H_{152}N_{22}O_{28}$	2098.45	2098.60	26.04
10–27;15P	$C_{99}H_{153}N_{22}O_{31}P_1$	2178.43	2178.11	25.04
10–27;18P	$C_{99}H_{153}N_{22}O_{31}P_1$	2178.43	2178.58	24.43
10–27;20P	$C_{99}H_{153}N_{22}O_{31}P_1$	2178.43	2177.75	25.65
10–27;15,18PP	$C_{99}H_{154}N_{22}O_{34}P_2$	2258.41	2258.74	23.87
10–27;15,20PP	$C_{99}H_{154}N_{22}O_{34}P_2$	2258.41	2257.89	24.20
10–27;18,20PP	$C_{99}H_{154}N_{22}O_{34}P_2$	2258.41	2258.15	24.09
10–27;15,18,20PPP	$C_{99}H_{155}N_{22}O_{37}P_3$	2338.39	2339.05	22.14
Fl-10-27;nP	$C_{120}H_{162}N_{22}O_{34}$	2456.77	2456.56	30.80
Fl-10-27;15P	$C_{120}H_{163}N_{22}O_{37}P_1$	2536.75	2536.51	28.83
Fl-10-27;18P	$C_{120}H_{163}N_{22}O_{37}P_1$	2536.75	2535.20	28.19
Fl-10-27;20P	$C_{120}H_{163}N_{22}O_{37}P_1$	2536.75	2536.75	30.53
Fl-10-27;15,18PP	$C_{120}H_{164}N_{22}O_{40}P_2$	2616.73	2615.54	27.83
Fl-10-27;15,20PP	$C_{120}H_{164}N_{22}O_{40}P_2$	2616.73	2617.28	28.10
Fl-10-27;18,20PP	$C_{120}H_{164}N_{22}O_{40}P_2$	2616.73	2616.34	27.96
Fl-10-27;15,18,20PPP	$C_{120}H_{165}N_{22}O_{43}P_3$	2696.71	2696.58	27.14
308-360;nP	$C_{266}H_{425}N_{77}O_{83}S_1$	6061.88	6061.24	20.25
308-360;315P	$C_{266}H_{426}N_{77}O_{86}P_1S_1$	6141.86	6145.70	20.20
Fl-308-360;nP	$C_{287}H_{435}N_{77}O_{89}S_1$	6420.20	6422.38	22.14
Fl-308-360;315P	$C_{287}H_{436}N_{77}O_{92}P_1S_1$	6500.18	6502.24	22.10

[a] C-18 RP-HPLC retention time (min) of the purified peptides in a linear gradient from 30% to 75% B over 45 min (10–27 fragments) and 15% to 55% B over 40 min (308–360 fragments) at the flow rate of 1.0 ml/min.

cleaved from the resin similarly to the procedure used for the unlabelled analogues.

The peptides were purified by RP-HPLC using an acetonitrile gradient for hydrophobic displacement and 0.1% TFA as the ion-pairing reagent in the eluent. Acidic solvents are widely used for the purification of peptide phosphate esters without difficulties. Indeed, we could accomplish the purification of the phosphoserine-containing p53 fragments without any difficulty. However, the peptides containing phosphorylated threonine residue showed increased instability in solution, even if they were stored in the freezer. To avoid decomposition of the threonine phosphate esters, the synthetic phosphopeptides were stored in lyophilized form at $-20\,^{\circ}C$ and were dissolved immediately before usage. In most cases a single purification step was not enough to obtain high quality products, so the purification was repeated once more by using a slightly different gradient. The yield was ~7%–12% and ~3%–5% for the unlabelled and labelled pure peptides, respectively. The relatively low overall yields are in line with the generally observed modest recovery of synthetic peptides after RP-HPLC purification. The analytical data of the peptides are summarized in Table 2.

The RP-HPLC elution order of the peptides was investigated in order to get insights into the change of hydrophobic/hydrophilic behaviour that might play roles in the interaction with the upstream and downstream regulatory proteins. Not surprisingly, the fluorescein-labelled set was eluted with a higher acetonitrile concentration than the unlabelled one. Within each set the triphosphate was eluted first, then the diphosphate esters, followed by the monophosphorylated and finally the unphosphorylated compounds. This elution order is due to the presence of the phosphate group that increases the hydrophilicity of the peptides. Comparing the retention times of the mono- or diphosphorylated isomers, the threonine-phosphates appeared to be the most hydrophilic and the Ser^{15} phosphates were eluted at lower acetonitrile concentration than the Ser^{20} phosphates. This latter observation is in good agreement with the algorithm of Browne *et al.* which predicts the retention behaviour of peptide fragments [34]. Comparison of 4–9 residue-long

Copyright © 2002 European Peptide Society and John Wiley & Sons, Ltd.

fragments flanking the two serines reveals that incorporation of a phosphate residue to Ser^{15} breaks a longer hydrophobic region than does phosphorylation of Ser^{20}. Supposedly, the shortest retention times of Thr^{18} phosphates are consequences of the more hydrophobic threonine side-chain itself. Building in a phosphate ester to this residue resulted in the most visible decrease in the retention time and therefore the most expressed increase in the local hydrophilic character.

Peptides representing the *N*-terminally extended tetramerization domain of p53 were synthesized in unphosphorylated and Ser^{315} phosphorylated forms. Sequences of these peptides are shown in Table 1. Peptides were synthesized on a continuous flow synthesizer in order to improve the efficacy of the coupling steps. HATU activation was used for the incorporation of the amino acids. To make sure that all coupling steps were fully executed, the coupling cycles were extended to 2–3 h, depending on the actual amino acid residues. Synthesis was performed on a 0.15 mmol scale until Pro^{316} when the resin was split to two equal parts and Ser^{315} was incorporated separately. One half of the resin was acylated with Fmoc-Ser(OtBu)-OH and continuing the peptide with the *N*-terminal seven amino acids, 308–360;nP was synthesized. The other half was double-coupled with Fmoc-Ser(PO_3HBzl)-OH and the synthesis of 308–360;315P was completed. Two third of the peptides (0.05 mmol) were detached from the resin using the same cleavage mixture as for the 10–27 fragments. After two subsequent HPLC purifications, the pure products were obtained at ~5%–7% yield. The rest of the peptides (0.025 mmol) were labelled with fluorescein on the resin as described for the 10–27 fragments. The yield of the synthesis after the second purification was ~3% for both Fl-308-360;nP and Fl-308-360;315P.

Interaction with Regulatory Proteins

The binding of *N*-terminally fluorescein-labelled p53 10–27 peptides to recombinant Mdm2 was studied by fluorescence polarization. While the use of a series of tracers prevented the assessment of the interaction in quantitative terms, it was clear that the Mdm protein bound to the unphosphorylated and all single phosphorylated peptides (15P, 18P and 20P) in submicromolar concentrations. Among the single phosphorylated analogues, 18P showed the lowest affinity to Mdm2, and 15P and 20P bound almost equally to the recombinant protein. When added at 1 μM concentration, the protein also bound to the double (15,18PP, 15,20PP and 18,20PP) as well as to the 15,18,20PPP triple phosphorylated p53 fragments over the level of the negative control *N*-terminally labelled antibacterial peptide, pyrrhocoricin.

The binding of the fluorescein-labelled 308–360 p53 fragments to DNA topoisomerase I was also studied by fluorescein polarization. The unphosphorylated and phosphorylated peptides showed almost identical affinity to the enzyme. Interestingly, fluorescein-labelled pyrrhocoricin also bound to the p53 tetramerization domain (data not shown). This is not surprising if we look at the peptide sequences. Pyrrhocoricin, as all antimicrobial peptides, is strongly positively charged, with the arginines and the lysine evenly distributed along the sequence. Conversely, the *C*-terminal third of the p53 308–360 fragment is strongly negatively charged, again, the glutamic acid and aspartic acid residues being interspersed with 2–3 uncharged residues. It is highly conceivable that attractive and well-positioned ionic forces promote the binding of pyrrhocoricin to the p53 tetramerization domain. Such non-specific interaction of the p53 *C*-terminus to other multiply charged biopolymers is a well-known phenomenon, and well represented by the non-specific DNA binding of the positively charged extreme *C*-terminal regulatory domain. None of the labelled peptides bound to the DsbA control protein to any degree (Figure 1).

Recognition by Phosphate-Specific Anti-p53 Antibodies

A more recently developed technique for studying site-specific protein phosphorylation involves the generation of phospho-specific antibodies, to use as probes for the detection of phosphorylated proteins under physiological conditions. The simplest and most powerful way for determining the specificity of the generated antibodies is a direct ELISA assay using a series of phosphopeptides as antigens. The unlabelled phosphopeptides containing amino acids 10–27 of p53 were used to characterize the specificity of anti-phospho-p53 Ser^{15} and Ser^{20} polyclonal and anti-phospho-p53 Ser^{15} monoclonal antibodies. In addition to the peptides, the antibody binding of highly phosphorylated p53 protein expressed in insect cells infected with recombinant baculovirus, and an unphosphorylated p53 variant expressed in *Escherichia coli* was also studied (Figure 2). The anti-phospho-p53 Ser^{15} polyclonal antibody

Copyright © 2002 European Peptide Society and John Wiley & Sons, Ltd.

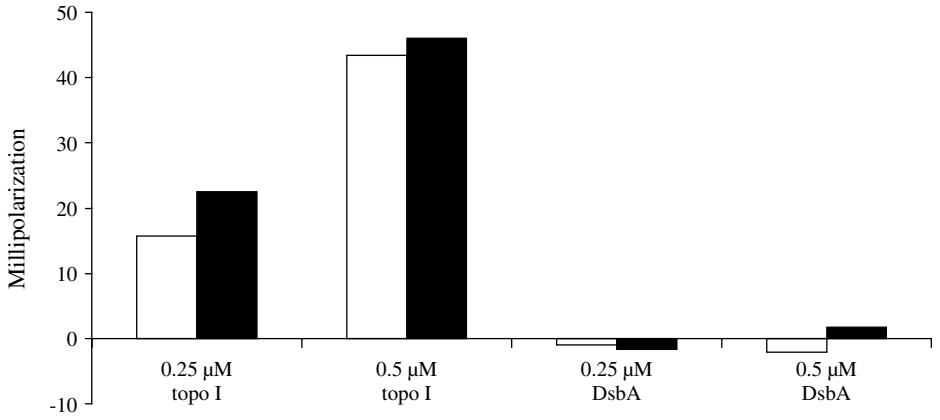

Figure 1 Binding of fluorescein-labelled p53 308–360 nonphosphorylated (□) and Ser^{315} phosphorylated (■) fragments to DNA topoisomerase I. DsbA protein was used as a negative control for the experiment.

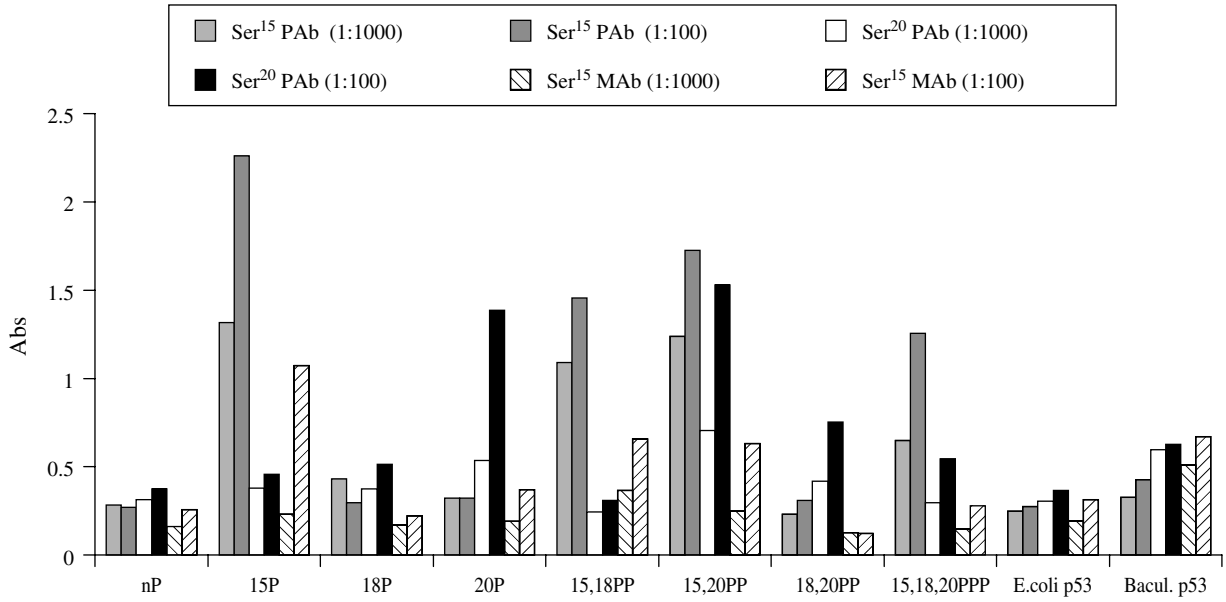

Figure 2 Recognition of p53 10–27 fragments by phosphate-specific anti-p53 antibodies, namely anti-phospho-p53 Ser^{15} polyclonal (Ser^{15} PAb), anti-phospho-p53 Ser^{20} polyclonal (Ser^{20} PAb), and anti-phospho-p53 Ser^{15} monoclonal (Ser^{15} MAb) antibodies. Antibodies were used at 1 : 1000 and 1 : 100 dilutions.

recognized the Ser^{15} monophosphorylated peptide, and bound equally well to the Ser^{15}-phosphate containing multiphosphorylated fragments (15,18PP, 15,20PP and 15,18,20PPP). However, it did not display affinity for those peptides in which Ser^{15} was unphosphorylated (nP, 18P, 20P, 18,20PP). The anti-phospho-Ser^{15} monoclonal antibody had similar specific binding characteristics. The monoclonal antibody showed lower affinity to all peptides but this might be only due to the different assay conditions and reagents and did not represent decreased specificity or efficacy. Similarly, the anti-phospho-Ser^{20} polyclonal antibody bound only to the phospho-Ser^{20} containing peptides (20P, 15,20PP, 18,20PP and 15,18,20PPP), and not to the others (nP, 15P, 18P and 15,18PP). All tested antibodies exhibited higher binding to phosphorylated p53 (expressed by baculovirus in insect cells) than to unphosphorylated p53 protein (expressed in *E. coli*).

Effect of Phosphorylation on the Conformation of the Tetramerization Domain

Phosphorylation of p53 was expected to influence the tetramer formation through altering the local

Copyright © 2002 European Peptide Society and John Wiley & Sons, Ltd.

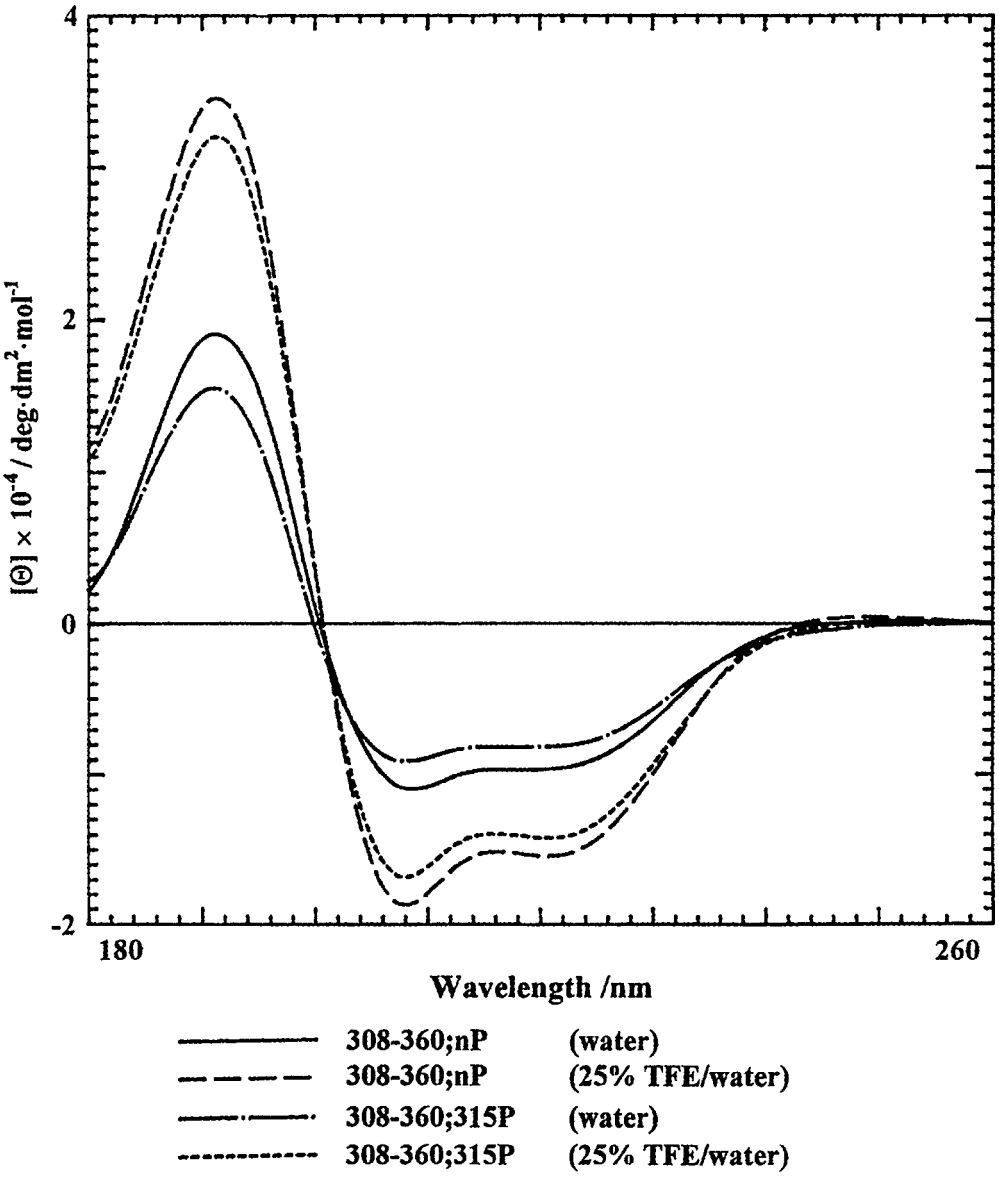

Figure 3 Circular dichroism spectra of the unphosphorylated and Ser^{315} phosphorylated p53 308–360 peptides in water and in 25% aqueous trifluoroethanol.

conformation of the peptide. These can be either local conformational effects around the phosphorylation site that would influence the *N*-terminal β-pleated sheet, or long range effects that would involve the *C*-terminal region of the α-helix. These conformational changes can be characterized by low or high resolution secondary structure analysis. As a low resolution technique, circular dichroism was used being a sensitive tool for determining stabilization or changes of the conformation of a protein or a peptide. CD studies of 308–360;nP and 308–360;315P peptides in trifluoroethanol solutions were done to obtain information on the effect of phosphorylation on the secondary structure of the peptides (Figure 3). While both peptides exhibited fairly helical structure in all solvents, the α-helicity increased with the trifluoroethanol content of the solvent. There was no significant difference between the secondary structure of the unphosphorylated and phosphorylated peptides. However, phosphorylation at Ser^{315} slightly destabilized the α-helix and reduced the α-helix content from 24% to 17% in water and from 52% to 45% measured in 25% TFE in water. (The α-helicity values were

Copyright © 2002 European Peptide Society and John Wiley & Sons, Ltd.

calculated at 208 nm according to Greenfield and Fasman [35].)

Oligomerization

Size-exclusion HPLC was used to assess the ability of the synthetic 308–360 fragments to form oligomers and to model the tetramer formation of the full-sized p53 protein. According to SE-HPLC, both the unphosphorylated and phosphorylated peptides readily formed tetramers at pH 7.1. Comparison of the retention times can be seen in Table 3. Either the tetramer formation was instant, or it occurred during the chromatography, but no monomer was detected, even if the peptides were loaded to the HPLC column from β-sheet breaker or denaturing agents, such as trifluoroacetic acid, dimethyl sulphoxide or 6 M guanidine hydrochloride solutions. At pH 7.1 no differences in the tetramer-forming ability of the unphosphorylated peptide and the Ser^{315}-phosphopeptide were found. When the chromatogram was run at pH 3.0 only the monomer could be detected for both peptides. This indicated that the oligomerization domain underwent a pH-dependent tetramerization process. Various buffer systems were evaluated between pH 3.0 and 7.1 in order to observe pH-dependent differences in the tetramerization process as regulated by the presence or absence of the phosphate group on Ser^{315}. In contrast to our expectations, no such difference could be detected in any of the solvent systems used.

DISCUSSION

The tumour suppressor p53 protein is present at extremely low levels in normally growing cells, and has a life span of mere minutes. p53 levels may be raised quickly by synthesis of more protein, and high levels are quickly reduced when synthesis abates [36]. The reduction of p53 levels in the cells proceeds through binding to its negative regulators, Mdm2 and Hdm2 [37], which proteins continuously shuttle between the nucleus and the cytoplasm where the proteasome-dependent degradation of p53 occurs [38,39]. Several p53 synthetic libraries, and an alanine substitution series were used to locate the Mdm2 binding site to the sequence TFSDLW (amino acids 18–23) [40]. *De novo* phosphorylation of p53 at Ser^{15} occurs in response to ionizing radiation [14,41], and using phosphate-specific polyclonal antibodies, Ser^{15} phosphorylated p53 appeared to be unable to bind Mdm2 [14]. Ser^{15} is located close enough to the Mdm2 binding site to accept the idea that phosphorylation interferes with Mdm2 interaction. Indeed, the first reports identified phosphorylated Ser^{15} as a negative regulator for Mdm2 and Hdm2 binding [9,42]. Using mono- and polyclonal antibodies other studies showed that DNA damage leads to the stabilization of p53 induced phosphorylation of different *N*-terminal amino acids [41,42], including Ser^{20}, which lies right in the middle of the Mdm2-binding element [43]. Soon Ser^{20} was identified as the key phosphorylated residue to inhibit Mdm2 binding [44] and it was claimed that substitution

Table 3 Comparison of the Retention Times of p53 308–360 Peptides with Molecular Weight Controls on Size-Exclusion HPLC

Peptide	Retention time (min)		MW (Da)
	pH 3.0	pH 7.1	
Thyroglobulin	10.8	11.2	670,000
IgG	11.6	12.6	158,000
Ovalbumin	15.3	14.5	44,000
Myoglobin	18.1	17.0	17,000
Vitamin B_{12}	21.3	20.8	1,350
Unrelated synthetic peptide 1	17.7		6,893
Unrelated synthetic peptide 2	18.5		5,184
Unrelated synthetic peptide 3	23.0		4,112
308–360;nP	18.6	14.7	6,061[a]
308–360;315P	19.0	15.2	6,141[a]

[a] Molecular weight of the monomer.

Copyright © 2002 European Peptide Society and John Wiley & Sons, Ltd.

of Ser^{20}, but not Ser^{15} was sufficient to abrogate p53 stabilization in response to both ionizing radiation or UV light [17,44,45]. However, normal cells and wild-type p53 expressing tumour cells show no differences in the phosphorylation pattern at Ser^{15} and Ser^{20} upon antinomycin D and camptotechin treatment [46], suggesting additional potential phosphorylation sites of p53 upon cancerous transformation of the cells. An additional hydroxyamino acid residue, Thr^{18} lies in the Mdm2-binding fragment of p53. In yet another report, Thr^{18} was identified as the residue whose phosphorylation blocks the interaction with Mdm2 [47].

The cellular co-activator p300/CBP protein family is also involved in the p53 transactivation function, through sharing the site of interaction with Mdm2 [14]. Moreover, p300 is thought to play a central role in mediating p53-dependent growth arrest [48,49]. Previously it was shown that phosphorylation at Ser^{15} stimulated p53 binding to p300/CBP *in vivo* and *in vitro* [50]. However, other reports claim that the role of phosphorylation of Thr^{18} and Ser^{20} is to stabilize p53–p300 complexes based on the observation that full-length p300 protein exhibits almost as low affinity for a Ser^{15} phosphorylated p53 fragment as for the unphosphorylated analogue [19]. A recent study, using competitive fluorescence polarization assay and synthetic p53 phosphopeptides, demonstrated that a Thr^{18} phosphorylated p53 fragment bound significantly tighter to p300 than an analogous Ser^{15} phosphorylated peptide [21]. However, this report does not provide any information on the effect of phosphorylation at Ser^{20}. In summary, the precise role of phosphorylation of the *N*-terminal p53 sites in recruitment of p300/CBP is still unclear.

An other crucial region of p53 is the *C*-terminally located tetramerization domain responsible for oligomerization that is essential for p53 function. Intriguingly, the binding site of DNA topoisomerase I partially overlaps with the *N*-terminus of the tetramerization domain [25]. Ser^{315}, a residue that is included in the topoisomerase I binding sequence, was previously shown to be phosphorylated by cdc2 kinase [26]. Phosphorylation of Ser^{315} can be a potential regulatory mechanism of DNA topoisomerase I binding and tetramerization of p53.

Methods based on fluorescence polarization are able to overcome the bias introduced by specific cell lines and the expression of mutated proteins. FP is increasingly used for studying peptide–protein interactions [51] and phosphopeptide binding to various biopolymers [52]. Direct DNA binding of the extreme *C*-terminal, basic regulatory domain of p53 (that follows the tetramerization domain) was investigated by using unphosphorylated and phosphorylated p53 peptides and 5′- fluorescein-labelled oligonucleotides [23]. In recent competition FP assays the interaction of phosphorylated p53 peptides and Mdm and p300 was studied [20,21]. However, these assays featured single fluorescein-labelled peptides (an unphosphorylated or a Ser^{15}-phosphorylated one), to which the competing power of test phosphopeptides was recorded. Indeed, in these studies not a single phosphopeptide–protein binding showed the traditional dose-response curve. A true comparison of K_d figures of protein binding to analogous peptides can only be obtained, if each peptide is independently labelled with fluorescein, and the individual binding constants are recorded. For these studies there is a need for a set of differentially phosphorylated fluorescein-labelled peptides representing the appropriate binding site of a given protein.

To demonstrate the feasibility of the synthesis of such highly complex reagents, in the current study we prepared a series of peptides comprising of amino acids 10–27, the Mdm2 and p300 binding site, with and without fluorescein-labelling, by step-by-step solid phase synthesis. We prepared the unphosphorylated fragment, as well as the Ser^{15}, Thr^{18} and Ser^{20} monophosphorylated, the three possible diphosphorylated and the triphosphorylated analogues. In addition, we prepared an unphosphorylated and a Ser^{315}-phosphorylated 53-mer corresponding to the *N*-terminally extended tetramerization domain of p53 with a similar synthetic strategy. Fluorescein-labelling of the *N*-terminus of the peptides, performed on the solid support using 5(6)-carboxy-fluorescein, resulted in the formation of an amide bond stable during acidic treatments. Repeated HPLC purification in 0.1% TFA containing eluent provided pure products in all cases. In contrast to the serine-phosphate esters that proved to be stable, the threonine-phosphates slowly decomposed when stored in solution.

Fluorescence polarization analysis of the 10–27 fragments revealed that phosphorylation at Thr^{18} decreased the Mdm2 binding compared with the unphosphorylated and the two other single phosphorylated peptides. This is in good agreement with recent findings on p53–Mdm2 interaction. Various groups reported that phosphorylation of Thr^{18} reduces binding of *N*-terminal p53 peptides to Mdm2. Regardless of whether the peptides are fluoresceinated and used in a competition binding

Copyright © 2002 European Peptide Society and John Wiley & Sons, Ltd.

experiment [21], or biotinylated p53 fragments are assayed in direct ELISA [19,43], 18P peptides form the least stable complexes with Mdm2. While we could support the findings of these studies in qualitative terms, our multiphosphorylated peptides did not give quantitative information about the binding affinity. As the number of phosphate groups increased, the fluorescence signal decreased, rendering the comparison of the millipolarization values meaningless. This observation may be due to the strong hydrophilic character of the relatively large phosphate groups. It is known from the crystal structure of the 109-amino-acid *N*-terminal domain of Mdm2 bound to a peptide from the transactivation domain of p53 that three hydrophobic amino acids of p53, Phe^{19}, Trp^{23} and Leu^{26} are the key recognition elements [13]. A possible explanation of our low millipolarization values observed for the multiphosphorylated peptides was that the large hydrophilic phosphate groups close to the Mdm2 interacting region of p53 disrupted the insert of the hydrophobic side chains into the Mdm2 cleft.

The set of unlabelled 10–27 peptides proved to be a powerful tool in analysing the phosphate specificity of anti-p53 monoclonal and polyclonal antibodies using direct ELISA. While anti-phospho-Ser^{15} antibodies recognized the Ser^{15} phosphorylated peptides, an anti-phospho-Ser^{20} antibody displayed affinity for those peptides in which Ser^{20} was introduced as a phosphate ester. This binding assay documents not only the phosphate specificity of the characterized antibodies, but also the high quality and integrity of our complex synthetic phosphopeptides. Based on the presented ELISA data, the phosphate group did not migrate from one residue to another, even if the Thr^{18} phosphopeptides proved to be chemically unstable during storage.

According to our fluorescence polarization analysis, the fluorescein-labelled Ser^{315} phosphorylated peptide corresponding to the *N*-terminally extended tetramerization domain of p53, bound to DNA topoisomerase I with slightly higher affinity than the unphosphorylated analogue. However, the difference was not high enough to draw quantitative conclusions from this single experiment and further investigations are needed to provide additional evidence to this finding.

CD analysis of the unlabelled 308–360 analogues of p53 revealed that both peptides exhibited fairly helical structure and no major difference in the secondary structure could be observed upon phosphorylation. Lee *et al.* reported similar observations by examining the structure of the 303–360 p53 fragment by NMR [53]. In contrast to these results, Sakamoto *et al.* detected an increase in the α-helix content upon phosphorylation at Ser^{315} using CD spectroscopy [54]. However, this study involved a *C*-terminally extended tetramerization domain peptide corresponding to amino acids 303–393 suggesting that the effect of phosphorylation might have been due to an interaction with the highly positively charged regulatory domain located at the extreme *C*-terminus.

Size-exclusion HPLC indicated that the synthetic 308–360 fragments underwent pH-dependent tetramerization as expected from the highly hydrophilic nature of the two terminal domains of the full-sized p53 protein. Both the unphosphorylated and phosphorylated 308–360 peptides formed tetramers at pH 7.1 but appeared to be in a monomeric state at pH 3.0. While the synthetic peptides might truly represent an independently functioning unit of a multi-domain structured protein during the oligomerization experiment, SE-HPLC did not show a difference between the tetramer forming abilities of the unphosphorylated and Ser^{315} phosphorylated fragments. This finding is in good agreement with analytical ultracentrifugation of p53 fragments, published by Sakaguchi *et al.* demonstrating that phosphorylation does not change the oligomeric state of synthetic p53 peptides [55].

The study reported here demonstrates not only the possibility of the synthesis of phosphopeptides carrying multiple substitutions as well as other modifications or the preparation of protein fragments longer than 50 amino acids in doubly modified forms, but also the ability of appropriately designed peptides to model full-length proteins that are organized in independently functioning domains.

Acknowledgements

The authors would like to thank Dr Gabor K. Toth for critical reading of the manuscript. This study was supported by NIH Grant GM 55860.

REFERENCES

1. Lu X, Lane DP. Differential induction of transcriptionally active p53 following UV or ionizing radiation: defects in chromosome instability syndromes? *Cell* 1993; **75**: 765–778.

Copyright © 2002 European Peptide Society and John Wiley & Sons, Ltd.

2. Lowe SW, Ruley HE. Stabilization of the p53 tumor suppressor is induced by adenovirus 5 E1A and accompanies apoptosis. *Genes Dev.* 1993; **7**: 535–545.
3. Graeber TG, Peterson JF, Tsai M, Monica K, Fornace AJ Jr, Giaccia AJ. Hypoxia induces accumulation of p53 protein, but activation of a G_1-phase checkpoint by low-oxygen condition is independent of p53 status. *Mol. Cell Biol.* 1991; **14**: 6264–6277.
4. Cross SM, Sanchez CA, Morgan CA, Schimke MK, Ramel S, Idzerda RL, Raskind WH, Reid BJ. A p53-dependent mouse spindle checkpoint. *Science* 1995; **267**: 1353–1356.
5. Amundson SA, Myers TG, Fornace AJ Jr. Roles for p53 in growth arrest and apoptosis: putting on the brakes after genotoxic stress. *Oncogene* 1998; **17**: 3287–3299.
6. Levine AJ. p53, the cellular gatekeeper for growth and division. *Cell* 1997; **88**: 323–331.
7. Oren M. Lonely no more: p53 finds its kin in a tumor suppressor haven. *Cell* 1997; **90**: 829–832.
8. Agarwal ML, Taylor WR, Chernov MV, Chernova OB, Stark GR. The p53 network. *J. Biol. Chem.* 1998; **273**: 1–4.
9. Prives C. Signaling to p53: breaking the MDM2-p53 circuit. *Cell* 1998; **95**: 5–8.
10. Giaccia AJ, Kastan MB. The complexity of p53 modulation: emerging patterns from divergent signals. *Genes Dev.* 1998; **12**: 2973–2983.
11. Ljungman M. Dial 9-1-1 for p53: mechanism of p53 activation by cellular stress. *Neoplasia* 2000; **2**: 208–225.
12. Pietenpol JA, Tokino T, Thiagalingam S, el-Deiry WS, Kinzler KW, Vogelstein B. Sequence-specific transcriptional activation is essential for growth suppression by p53. *Proc. Natl Acad. Sci. USA* 1994; **91**: 1998–2002.
13. Kussie PH, Gorina S, Marechal V, Elenbaas B, Moreau J, Levine AJ, Pavletich NP. Structure of the MDM2 oncoprotein bound to the p53 tumor suppressor transactivation domain. *Science* 1996; **274**: 948–953.
14. Shieh S-Y, Ikeda M, Taya Y, Prives C. DNA damage-induced phosphorylation of p53 alleviates inhibition by MDM2. *Cell* 1997; **91**: 325–334.
15. Pise-Masison CA, Radonovich MF, Sakaguchi K, Appella E, Brady JN. Phosphorylation of p53: a novel pathway for p53 inactivation in human T-cell lymphotropic virus type 1-transformed cells. *J. Virol.* 1998; **72**: 6348–6355.
16. Lambert PF, Kashanchi F, Radonovich MF, Shiekhattar R, Brady JN. Phosphorylation of p53 serine 15 increases interaction with CBP. *J. Biol. Chem.* 1998; **273**: 33048–33053.
17. Ashcroft M, Kubbutat MH, Vousden KH. Regulation of p53 function and stability by phosphorylation. *Mol. Cell Biol.* 1999; **19**: 1751–1758.
18. Dumaz N, Milne DM, Jardine LJ, Meek DW. Critical roles for the serine 20, but not the serine 15, phosphorylation site and for the polyproline domain in regulating p53 turnover. *Biochem. J.* 2001; **359**: 459–464.
19. Dornan D, Hupp TR. Inhibition of p53-dependent transcription by BOX-I phospho-peptide mimetics that bind to p300. *EMBO Rep.* 2001; **2**: 139–144.
20. Sakaguchi K, Saito S, Higashimoto Y, Roy S, Anderson CW, Appella E. Damage-mediated phosphorylation of human p53 threonine 18 through a cascade mediated by a casein 1-like kinase. Effect on Mdm2 binding. *J. Biol. Chem.* 2000; **275**: 9278–9283.
21. Kar S, Sakaguchi K, Shimohigashi Y, Samaddar S, Banerjee R, Basu G, Swaminathan V, Kundu TK, Roy S. Effect of phosphorylation on the structure and fold of transactivation domain of p53. *J. Biol. Chem.* 2002; **277**: 15579–15585.
22. Zhang Y, Xiong YA. p53 amino-terminal nuclear export signal inhibited by DNA damage-induced phosphorylation. *Science* 2001; **292**: 1910–1915.
23. Hoffmann R, Craik DJ, Pierens G, Bolger RE, Otvos L Jr. Phosphorylation of the *C*-terminal sites of human p53 reduces non-sequence-specific DNA binding as modelled with synthetic peptides. *Biochemistry* 1998; **37**: 13755–13764.
24. Larsen AK, Gobert C, Gilbert C, Markovits J, Bojanowski K, Skladanowski A. DNA topoisomerases as repair enzymes: mechanism(s) of action and regulation by p53. *Acta Biochim. Pol.* 1998; **45**: 535–544.
25. Gobert C, Skladanowski A, Larsen AK. The interaction between p53 and DNA topoisomerase I is regulated differently in cells with wild-type and mutant p53. *Proc. Natl Acad. Sci. USA* 1999; **31**: 10355–10360.
26. Wang Y, Prives C. Increased and altered DNA binding of human p53 by S and G2/M but not G1 cyclin-dependent kinases. *Nature* 1995; **376**: 88–91.
27. Li L, Ljungman M, Dixon JE. The human Cdc14 phosphatases interact with and dephosphorylate the tumor suppressor protein p53. *J. Biol. Chem.* 2000; **275**: 2410–2414.
28. Halazonetis TD, Davies LJ, Kandil AN. Wild-type p53 adopts a 'mutant'-like conformation when bound to DNA. *EMBO J.* 1993; **12**: 1021–1028.
29. Sakamoto H, Lewis MS, Kodama H, Appella E, Sakaguchi K. Specific sequences from the carboxyl terminus of human p53 gene product form anti-parallel tetramers in solution. *Proc. Natl Acad. Sci. USA* 1994; **91**: 8974–8978.
30. Clubb RT, Omichinski JG, Sakaguchi K, Appella E, Gronenborn AM, Clore GM. Backbone dynamics of the oligomerization domain of p53 determined from ^{15}N NMR relaxation measurements. *Protein Sci.* 1995; **4**: 855–862.
31. McCoy M, Stavridi ES, Waterman JLF, Wieczorek AM, Opella SJ, Halazonetis TD. Hydrophobic side-chain size is a determinant of the three-dimensional structure of the p53 oligomerization domain. *EMBO J.* 1997; **16**: 6230–6236.

Copyright © 2002 European Peptide Society and John Wiley & Sons, Ltd.

32. Weber PJA, Bader JE, Folkers G, Beck-Sickinger AG. A fast and inexpensive method for *N*-terminal fluorescein-labeling of peptides. *Bioorg. Med. Chem. Lett.* 1998; **8**: 597–600.
33. Kaiser E, Colescott RL, Bossinger CD, Cook PI. Color test for detection of free terminal amino groups in the solid-phase synthesis of peptides. *Anal. Biochem.* 1970; **34**: 595–598.
34. Browne CA, Bennett HP, Solomon S. The isolation of peptides by high-performance liquid chromatography using predicted elution positions. *Anal. Biochem.* 1982; **124**: 201–208.
35. Greenfield N, Fasman GD. Computed circular dichroism spectra for the evaluation of protein conformation. *Biochemistry* 1969; **8**: 4108–4116.
36. Midgley CA, Lane DP. p53 protein stability in tumor cells is not determined by mutation but is dependent on Mdm2 binding. *Oncogene* 1997; **15**: 1179–1189.
37. Haupt Y, Maya R, Kazaz A, Oren M. Mdm2 protein promotes rapid degradation of p53. *Nature* 1997; **387**: 296–299.
38. Roth J, Dobbelstein M, Freedman DA, Shenk T, Levine AJ. Nucleo-cytoplasmic shuttling of the hdm2 oncoprotein regulates the levels of the p53 protein via a pathway used by the human immunodeficiency virus rev protein. *EMBO J.* 1998; **17**: 553–564.
39. Tao W, Levine AJ. P19(ARF) stabilizes p53 by blocking nucleo-cytoplasmic shuttling of Mdm2. *Proc. Natl Acad. Sci. USA* 1999; **96**: 6937–6941.
40. Picksley SM, Vojtesek B, Sparks A, Lane DP. Immunochemical analysis of the interaction of p53 with MDM2; fine mapping of the MDM2 binding site on p53 using synthetic peptides. *Oncogene* 1994; **9**: 2523–2529.
41. Siliciano JD, Canman CE, Taya Y, Sakaguchi K, Appella E, Kastan MB. DNA damage induces phosphorylation of the amino terminus of p53. *Genes Dev.* 1997; **11**: 3471–3481.
42. Meek DW. New developments in the multi-site phosphorylation and integration of stress signalling at p53. *Int. J. Radiat. Biol.* 1998; **74**: 729–737.
43. Craig AL, Burch L, Vojtesek B, Mikutowska J, Thompson A, Hupp TR. Novel phosphorylation sites of human tumour suppressor protein p53 at Ser20 and Thr18 that disrupt the binding of mdm2 (mouse double minute 2) protein are modified in human cancers. *Biochem. J.* 1999; **342**: 133–141.
44. Chehab NH, Malikzay A, Stavridi ES, Halazonetis TD. Phosphorylation of Ser-20 mediates stabilization of human p53 in response to DNA damage. *Proc. Natl Acad. Sci. USA* 1999; **96**: 13777–13782.
45. Unger T, Juven-Gershon T, Moallem E, Berger M, Sionov RV, Lozano G, Oren M, Haupt Y. Critical role for Ser20 of human p53 in the negative regulation of p53 by Mdm2. *EMBO J.* 1999; **18**: 1805–1814.
46. Ashcroft M, Taya Y, Vousden KH. Stress signals utilize multiple pathways to stabilize p53. *Mol. Cell Biol.* 2000; **20**: 3224–3233.
47. Dumaz N, Milne DM, Meek DW. Protein kinase CK1 is a p53-threonine 18 kinase which requires prior phosphorylation of Ser15. *FEBS Lett.* 1999; **463**: 312–316.
48. Avantaggiati ML, Ogryzko V, Gardner K, Giordano A, Levine AS, Kelly K. Recruitment of p300/CBP in p53-dependent signal pathways. *Cell* 1997; **89**: 1175–1184.
49. Yuan Z-M, Huang Y, Ishiko T, Nakada S, Utsugisawa T, Shioya H, Utsugisawa Y, Yokoyama K, Weichselbaum R, Shi Y, Kufe D. Role for p300 in stabilization of p53 in response to DNA damage. *J. Biol. Chem.* 1999; **274**: 1883–1886.
50. Dumaz N, Meek DW. Serine15 phosphorylation stimulates p53 transactivation but does not directly influence interaction with HDM2. *EMBO J.* 1999; **18**: 7002–7010.
51. Pin SS, Kariv I, Graciani NR, Oldenburg KR. Analysis of protein–peptide interaction by a miniaturized fluorescence polarization assay using cyclin-dependent kinase 2/cyclin E as a model system. *Anal. Biochem.* 1999; **275**: 156–161.
52. Coffin J, Latev M, Bi X, Nikiforov TT. Detection of phosphopeptides by fluorescence polarization in the presence of cationic polyamino acids: application to kinase assays. *Anal. Biochem.* 2000; **278**: 206–212.
53. Lee W, Harvey TS, Yin Y, Yau P, Litchfield D, Arrowsmith CH. Solution structure of the tetrameric minimum transforming domain of p53. *Nature Struct. Biol.* 1994; **1**: 877–890.
54. Sakamoto H, Kodama H, Higashimoto Y, Kondo M, Lewis MS, Anderson CW, Appella E, Sakaguchi K. Chemical synthesis of phosphorylated peptides of the carboxy-terminal domain of human p53 by a segment condensation method. *Int. J. Pept. Protein Res.* 1996; **48**: 429–442.
55. Sakaguchi K, Sakamoto H, Xie D, Erickson JW, Lewis MS, Anderson CW, Appella E. Effect of phosphorylation on tetramerization of the tumor suppressor protein p53. *J. Protein Chem.* 1997; **16**: 553–556.

Copyright © 2002 European Peptide Society and John Wiley & Sons, Ltd.